

# Low-threshold and High-speed Quantum-dot Microring Lasers on Silicon

Chong Zhang, Di Liang, Geza Kurzeveil, Raymond G. Beausoleil  
System Architecture Lab, Hewlett Packard Labs, Hewlett Packard Enterprise  
Palo Alto, CA 94304 – United States  
Tel: +18058866378, e-mail: chong.zhang@hpe.com

## ABSTRACT

We report the demonstration of the first hybrid quantum-dot (QD) microring lasers integrated on silicon. By transferring 1.3  $\mu\text{m}$  InAs/GaAs QD gain layers to prepatterned SOI substrate, low threshold-current hybrid ring lasers are realized on silicon. High-speed direct current modulation of over 10 Gbps is achieved as well.

**Keywords:** Quantum dot laser, hybrid integration, direct laser modulation, silicon photonics.

## 1. INTRODUCTION

Next-generation high-performance computers (HPCs) demand few Tb/s communication bandwidth between switch hubs and hundreds of Gb/s bandwidth between nodes and hubs to overcome the challenge with rapid growing traffic. Integrated photonic interconnect is believed to be the solution for its advantages in high volume, low power and low cost, and high capacity with unique signal multiplexing techniques, e.g. wavelength division multiplexing (WDM). We have been developing a number of key photonic components, including low-threshold hybrid quantum well (QWs) microring lasers on silicon [1], and a new concept of integrated hybrid metal-oxide-semiconductor (MOS) capacitor for wavelength tuning [2] and data modulation. To further reducing device power consumption and enhancing high-temperature robustness, we have successfully transferred QD laser epitaxial material on this platform recently [3].

QDs lasers have drawn great attention due to their tolerance to material defects and higher radiative recombination efficiency at high temperature compared with QWs [3]. High-quality QDs materials can be epitaxially grown on silicon wafer and record-high laser output power [4] and sub-mA threshold lasing [5] have been reported, however, thick buffer layers still pose a big challenge to interact with silicon photonics. In this paper, we for the first time demonstrate the QD microring lasers on silicon with hybrid integration approach. Low threshold currents down to 2.5 mA at room temperature were achieved in devices with 50  $\mu\text{m}$  in diameter. The RF performance as well as the direct modulation bandwidth are investigated and discussed in this paper.

## 2. DEVICE DESIGN

The device structure of the hybrid microring lasers is schematically shown in Fig. 1. The microring laser mainly consists of two parts: silicon waveguide (WG) and III-V mesa. The ring waveguide on silicon defines the laser cavity, while the bus waveguide couples out the emitted light from the ring. The III-V mesa consists of multiple layers of InAs/GaAs QDs with center photoluminescence wavelength around 1.3  $\mu\text{m}$ . p- and n-doped GaAs/AlGaAs layers sandwiches the QDs stack to confine the optical mode as well as to offer electrode contacts. Intentional lateral offset between III-V mesa with silicon ring waveguide and curved bus waveguide are designed to adjust the optical coupling strength between ring and bus waveguide which represents the mirror loss of the laser cavity.

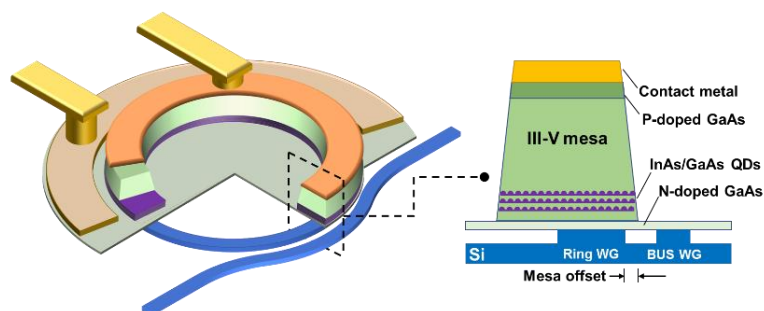


Figure 1. Diagram of hybrid microring laser on silicon and its cross-section structure.

The laser chip was fabricated with a complementary metal-oxide-semiconductor (CMOS) compatible process. The silicon-on-insulator (SOI) used this work has a 400 nm device layer and 1  $\mu\text{m}$  buried-oxide layer. Unlike the previous reported self-aligned fabrication process [6], the silicon waveguide on the SOI substrate was

firstly patterned and etched, together with the grating couplers (GCs) used for coupling the light out with a single-mode fiber. Then the GaAs substrate with QDs layer stack was bonded to the SOI substrate followed with substrate removal. The standard III-V process defines the III-V mesa, n- and p- contact metallization, followed with passivation, via etch and probe-metal contact. Fig. 2(a) shows the scanning electron microscopic (SEM) image of the ring mesa after dry etch, with the p-type contact metal on top of the mesa. Fig. 2(b) shows the top-view of the device after process. The III-V mesa width is 5  $\mu\text{m}$ , and the ring diameter is 50  $\mu\text{m}$ . Fig. 2(c) shows the cross-section after focus ion beam etching across the bus waveguide. The dry etch-resulted sloped sidewall of the III-V mesa contributes to a higher optical coupling strength to the bus waveguide. Two Si GCs at the end of the bus waveguide are used to collect lasers' clock-wise (CW) and counterclockwise (CCW) output.

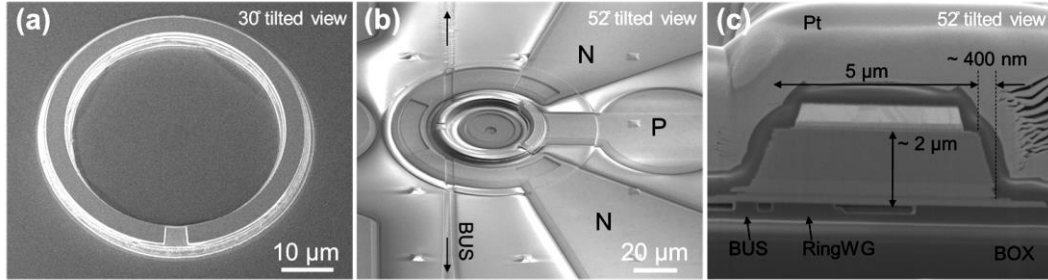


Figure 2. SEM images of the (a) III-V ring mesa, (b) the device after process, and (c) cross-section at the BUS waveguide.

### 3. MEASUREMENT RESULTS

The device characterizations were performed at room temperature without active temperature control. The microring designs tested in this work have 50  $\mu\text{m}$  diameter and 5  $\mu\text{m}$  wide III-V mesa, but different mesa lateral offset and bus coupling length. Fig. 3(a) shows the light-current-voltage (LIV) curve of a microring laser under continuous-wave (cw) pumping. With optimized electrode contact, the series resistance of the microring laser is as low as 16  $\Omega$ . Low threshold current was achieved around 2.5 mA at room temperature, equivalent to a 320 A/cm<sup>2</sup> threshold current density. Reasonable optical power over 0.6 mW was out-emitted into the bus waveguide in the CCW direction. The ripples on the LI curve represents both modes competition among longitude modes and the direction switch between CW and CCW directions. The output power didn't show thermal rollover until 35 mA (14 $\times$  threshold) injection, indicating much better temperature stability in QD gain region. The lasing spectrum at 31.63 mA in Fig. 3(b) shows excellent extinction ratio of 50 dB (limited by the instrument) for the primary lasing mode and a high side-mode suppression ratio (SMSR) of 33 dB over the O band. Due to large and relatively flat optical gain envelop in QD gain region and reflection feedback from the imperfect GCs designs, multiple spectral mode lasing with <10 dB SMSR and free spectral range  $\sim$ 3 nm is common in many injection levels (Fig. 4(c)). Smaller device dimension will help to achieve >30 dB SMSR in more injection range, which is equivalent to single-mode operation. A small wavelength drifting coefficient of 0.037 nm/mW because of self-heating is observed as well.

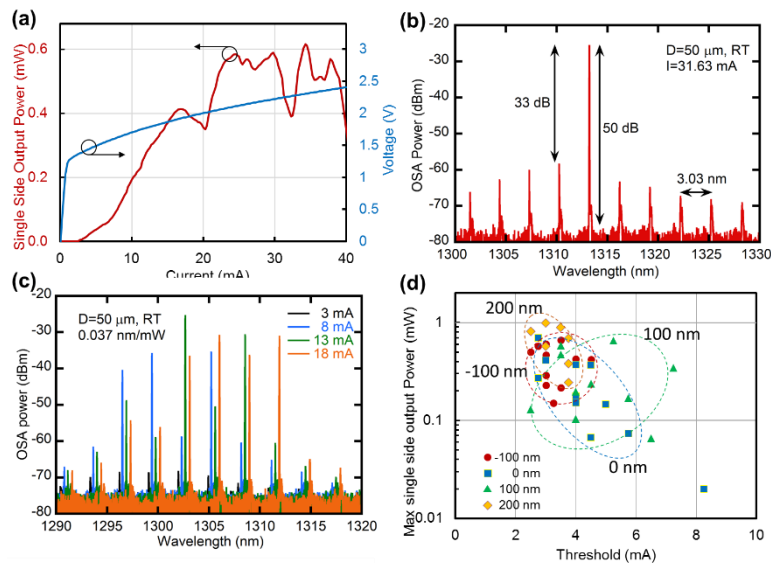


Figure 3. (a) LIV curves of 50  $\mu\text{m}$  hybrid QD ring laser, and (b) (c) the output spectrum under different injection current. (d) Threshold current – maximum power analysis of QD ring lasers with different mesa offset.

We also tested different microring structure designs with different mesa offset, and bus waveguide coupling length. Those devices are fabricated side by side on the same chip, showing high process yield but different lasing performance. Their maximum single side output power and threshold current are analyzed in Fig. 3(c). Depending on the curved section length in bus waveguide, i.e., effective mirror loss, lasing took place between 2.5 to 8 mA with maximum output single-side output power from tens of  $\mu\text{W}$  to 1 mW. Due to the sloped sidewall of the III-V mesa, the optimum mesa offset distance is either -100 nm or 200 nm, which have both lower threshold current and higher output power. This indicates that these two configurations have lower optical mode loss at the ring-bus coupler, that is equivalent to a lower cavity leakage loss that is preferred by the limited gain value from the thin QD layers.

The direct modulation bandwidth of the hybrid ring lasers was characterized at uncooled circumstance with a 20 GHz lightwave component analyzer. The frequency response of the 50 QD microring laser is shown in Fig. 4(a). The 3-dB bandwidth is about 3 GHz under small signal condition with 25 mA injection current, and 6 GHz with 35 mA injection current. The communication test was performed with an external high-speed photodetector. A semiconductor optical amplifier and optical filter were used to compensate the coupling loss from the GCs. With  $2^7-1$  non-return-to-zero pseudorandom binary sequence data input, clear open eye was seen up to 10 Gb/s data rate by directly modulating the laser driving current, as shown in Fig. 4(b). No signal pre-emphasis or equalizer was used in the communication test.

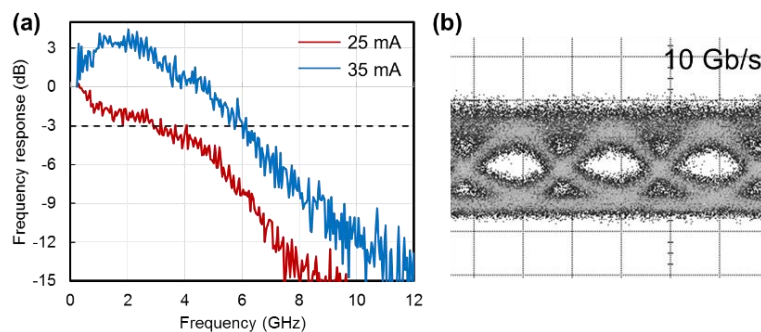


Figure 4. (a) Frequency response of QDs microring under direct current modulation, and (b) eye diagram of direct modulation of the QDs microring at 10 Gb/s.

#### 4. CONCLUSIONS

To our best knowledge, this is the first time that the QDs microring lasers are demonstrated on silicon with the hybrid integration approach. Those microring lasers show low threshold current of few mA and high output power of around 1 mW. High speed current modulation up to 10 Gb/s data rate was also demonstrated, which provides a promising on-chip laser solution in the node-to-node WDM links in future HPCs and other datacom applications.

#### ACKNOWLEDGEMENTS

The authors thank the Nanofabrication facility at University of California Santa Barbara for the support on device process.

#### REFERENCES

- [1] D. Liang, M. Fiorentino, R. G. Beausoleil, *Silicon Photonics III: Systems and Applications*, Chap. 18, Springer Science & Business Media, 2016.
- [2] D. Liang, *et al.*: Integrated finely tunable microring laser on silicon, *Nat. Photonics*, vol. 10, pp. 719, Nov. 2016.
- [3] Geza, *et al.*: Robust hybrid quantum dot laser for integrated silicon photonics, *Opt. Express*, vol. 24, pp. 16167, Jul. 2016.
- [4] A. Liu, *et al.*: High performance continuous wave 1.3  $\mu\text{m}$  quantum dot lasers on silicon, *Appl. Phys. Lett.*, vol. 104, pp. 041104, Jan. 2014.
- [5] Y. Wan, *et al.*: 1.3  $\mu\text{m}$  submilliamp threshold quantum dot micro-lasers on Si, *Optica*, vol. 4, pp. 940, Aug. 2017.
- [6] C. Zhang, *et al.*: Thermal management of hybrid silicon ring lasers for high temperature operation, *IEEE J. Sel. Top. Quantum Electron*, vol. 21, pp. 385, Nov. 2015.